

# Simulation of current-voltage characteristics of graphene field effect transistor (GFET)

• Dinh Sy Hien

University of Science, VNU-HCM

(Manuscript received on December 27<sup>th</sup> 2012, accepted on October 11<sup>st</sup> 2013)

## ABSTRACT

Graphene has been one of the most vigorously studied research materials. We have developed a program for simulation of graphene field effect transistor (GFET). In this work, we use the simulation program to explore the performance of graphene FET. The simple model of the graphene FET is based on non-equilibrium Green's function

method and first is implemented by using graphic user interface of Matlab. The current-voltage characteristics of the GFET and affects of channel materials, gate materials, size of graphene FET, temperature on the characteristics are explored.

**Keywords:** Graphene, Graphene FET, non-equilibrium Green's function, current-voltage characteristics.

## INTRODUCTION

Graphene [1-8] has been one of the most vigorously studied research materials since its inception in 2004. There has been a lot of study focused on transport properties of graphene [9-12]. Many issues related to transport properties of graphene field-effect transistors (FETs). Experimental [13-16] and theoretical [17-21] studies have shown that even though being a gapless semi-metallic material, a graphene FET shows saturating current-voltage behaviors.

In previous studies [17-21], to describe semi-classical transport of graphene FET at a channel length that a semi-classical Boltzmann transport equation (BTE) is solved self consistently with Poisson equation. Monte-Carlo method and numerical solutions of solving BTE have been implemented, they are limited to two-dimensional k-space, which assumes a homogeneous material and therefore it has

limitations to describe transport properties in the graphene transistor accurately.

In this work, to describe transport behaviors of graphene FET at channel length that quantum mechanical Schrodinger wave equation is solved self consistently with Poisson equation. The non-equilibrium Green's function (NEGF) method [22], that used commonly for nanoscale devices, has been implemented by using graphic user interface (GUI) of Matlab as discussed in detail later.

In the work, we start with an introduction to a top-gated graphene experimental field effect transistor, modeling and simulation method. In the second section, we look more into details of graphene field effect transistor (GFET). Finally, we discuss typical simulations of current-voltage characteristics in graphene FET by non-equilibrium Green's function method using GUI of Matlab.

**MATERIALS AND METHODS**

**Materials, Modeling and Simulation Method**

Top-gated graphene FET as shown in Fig. 1 were simulated. The normal device has a top gate insulator of Al<sub>2</sub>O<sub>3</sub> [23]. Fabrication of GFET can be briefly described as follows. Graphene monolayer flakes are exfoliated from bulk natural graphite crystals by the micromechanical cleavage. The substrate consists of a highly-doped, n-type Si(100) wafer with an arsenic doping concentration of N<sub>D</sub> > 10<sup>20</sup> cm<sup>-3</sup>, on which a 300 nm-thick SiO<sub>2</sub> layer is grown by thermal oxidation. Metal contacts on the sample is defined by using electron beam lithography

(EBL) followed by a 50 nm-thick metal (Ni) layer evaporation and a lift-off process. The device is transferred to electron beam evaporator vacuum chamber to deposit the Al nucleation layer. The thickness of Al layer is 1-2 nm. Then, the samples are moved to the atomic layer deposition (ALD) chamber and go through 167 cycles of Al<sub>2</sub>O<sub>3</sub> deposition resulting a 15 nm-thick Al<sub>2</sub>O<sub>3</sub> film deposition. A 50 nm-thick Ni top-gate electrode is subsequently fabricated using e-beam lithography, metal deposition and lift-off process. A graphene FET with 6.6 μm source-drain separation and 2.4 μm top-gate length is shown in Fig. 1 [23].

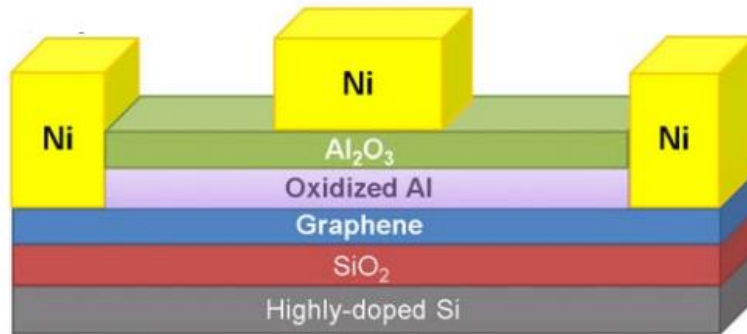


**Fig. 1.** Structure of top gated graphene field-effect transistor [23] is used in our simulations.

The flow of current is due to the difference in potentials between the source and the drain, each of which is in a state of local equilibrium, but

maintained at different electro-chemical potentials  $\mu_{1,2}$  and hence with two distinct Fermi functions [22]:

$$f_1(E) \equiv f_0(E - \mu_1) = \frac{1}{\exp[(E - \mu_1)/k_B T] + 1} \tag{1}$$

$$f_2(E) \equiv f_0(E - \mu_2) = \frac{1}{\exp[(E - \mu_2)/k_B T] + 1} \tag{2}$$

by the applied bias V:  $\mu_2 - \mu_1 = -qV$ . Here, E- energy, k<sub>B</sub> - Boltzmann constant, T- temperature.

The density matrix is given by

$$\rho = \int_{-\infty}^{+\infty} \frac{dE}{2\pi} G^n(E) = \int_{-\infty}^{+\infty} \frac{dE}{2\pi} [A_1(E)f_1(E) + A_2(E)f_2(E)] \tag{3}$$

The current I<sub>D</sub> flows in the external circuit is given by Landauer formula:

$$I_D = (q/h) \int_{-\infty}^{+\infty} dE T(E) (f_1(E) - f_2(E)) \tag{4}$$

The quantity  $T(E)$  appearing in the current equation (4) is called the transmission function, which tells us the rate at which electrons transmit from the source to the drain contacts by propagating through the device. Knowing the device Hamiltonian  $[H]$  and its coupling to the

contacts described by the self-energy matrices  $\Sigma_{1,2}$ , we can calculate the current from (4). For coherent transport, one can calculate the transmission from the Green's function method, using the relation

$$T(E) = \text{Trace}[\Gamma_1 G \Gamma_2 G^+] = \text{Trace}[\Gamma_2 G \Gamma_1 G^+] \quad (5)$$

The appropriate NEGF equations are obtained:

$$G = [EI - H - \Sigma_1 - \Sigma_2]^{-1}, \Gamma_{1,2} = i[\Sigma_{1,2} - \Sigma_{1,2}^+], A_1(E) = G\Gamma_1 G^+, A_2(E) = G\Gamma_2 G^+, \quad (6)$$

$$G^n = [A_1]f(E) + [A_2]f(E), A \equiv i[G - G^+] = [A_1] + [A_2]$$

where  $H$  is effective mass Hamiltonian,  $I$  is an identity matrix of the same size,  $\Gamma_{1,2}$  are the broadening functions,  $A_{1,2}$  are partial spectral functions,  $A(E)$  are spectral function,  $G^n$  is correlation function. We use a discrete lattice with  $N$  points spaced by lattice spacing 'a' to calculate the eigenenergies for electrons in the channel.

## RESULTS AND DISCUSSION

The main goal of the project was to make a user-friendly simulation program that provides as much control as possible over every aspect of the simulation. Flexibility and ease of use are difficult to achieve simultaneously, but given the complexity of quantum device simulations became clear that both criteria were vital to program success. Consequently, graphic user

interface development was major part of the program.

We start by simulating  $I_D$ - $V_D$  characteristics of top-gated graphene FET. Figure 1 shows the schematic of the device used in our simulations. Top-gated graphene FET with two-dimensional graphene as the channel is simulated. The device is simulated with  $Al_2O_3$  as the dielectric which has been predicted to be one of the promising dielectrics for graphene FETs in recent experiment [23]. All the simulations have been done for channel length of GFET,  $L = 20$  nm.

Fig. 2 shows the  $I_D$ - $V_D$  characteristics of the graphene FET having the length of 20 nm versus different gate voltages. It can be noted that when the gate voltage is increased the saturated drain current exponentially increased. This behavior is in agreement with experimental results.

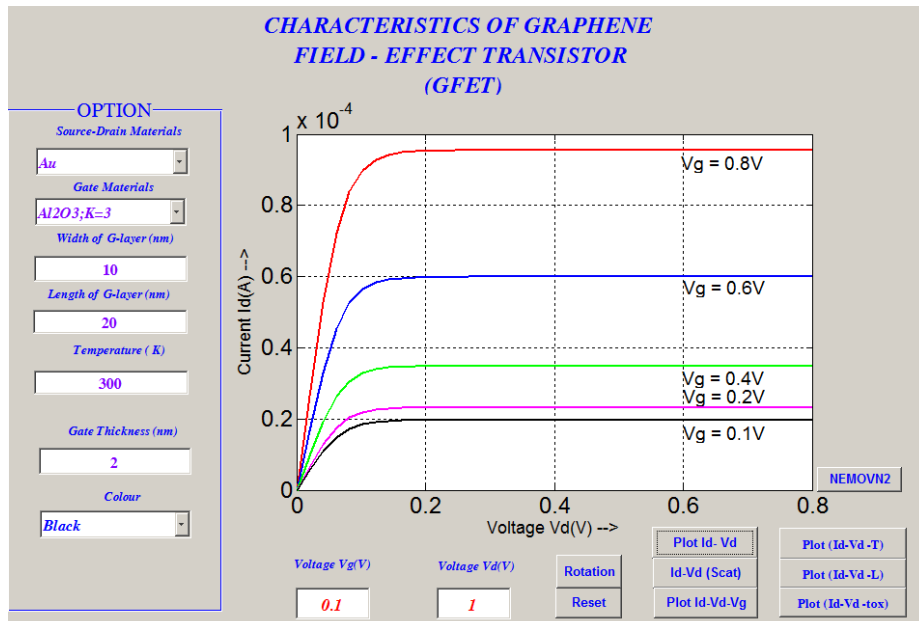


Fig. 2. The  $I_D$ - $V_D$  characteristics of the top gate graphene field-effect transistor at  $V_G = 0.1V, 0.2V, 0.4V, 0.6V, 0.8V$  (bottom to up).

Fig. 3 shows the  $I_D$ - $V_D$  characteristics of the top gate graphene FET having the length of 20 nm under ballistic transport and that with phonon scattering. It is shown that scattering can have an

appreciable affect on the ON-current. At  $V_{GS} = 0.8 V$ , the ON-current is reduced by 9% due to the phonon scattering.

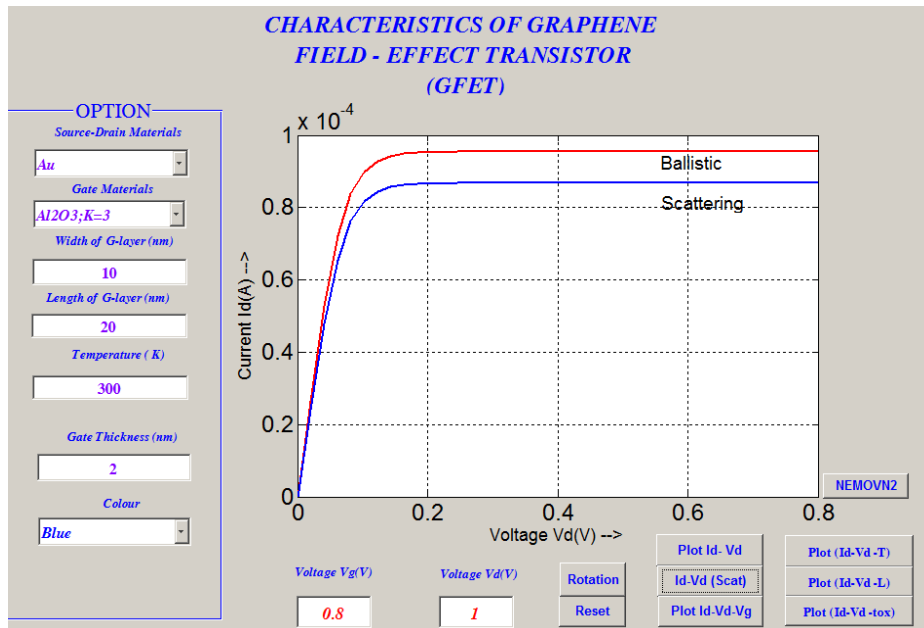


Fig. 3. The  $I_D$ - $V_D$  characteristics of the gate top graphene FET at  $V_G = 0.8V$  for ballistic (red line), scattering (black line), where the length of the gate is  $L_G=20$  nm.

Fig. 4 shows  $I_D$ - $V_D$  characteristics of graphene FET versus the gate voltage,  $V_G$ . When the gate voltage is small, the drain current is gradually increased. When the gate voltage is

greater than  $V_G = 0.3$  V, the drain current is exponentially increased. The modeling results agree well with experimental data.

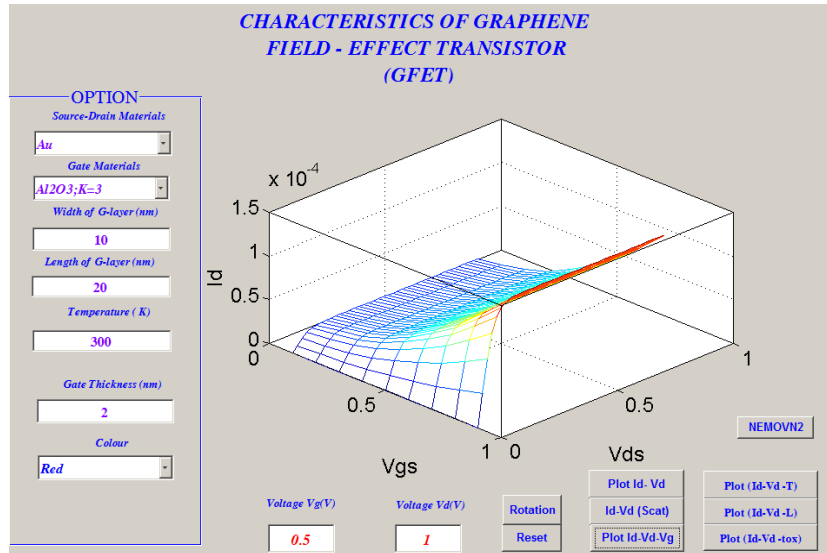


Fig. 4. The 3D plot of  $I_D$ - $V_D$  characteristics of the graphene FET vs  $V_G$ , where the length of the gate is  $L_G=20$  nm.

Fig. 5 shows the 3D plot of  $I_D$ - $V_D$  characteristics of the graphene FET versus the temperature, T. It can be noted that when the

temperature is increased the saturated drain current is gradually decreased.

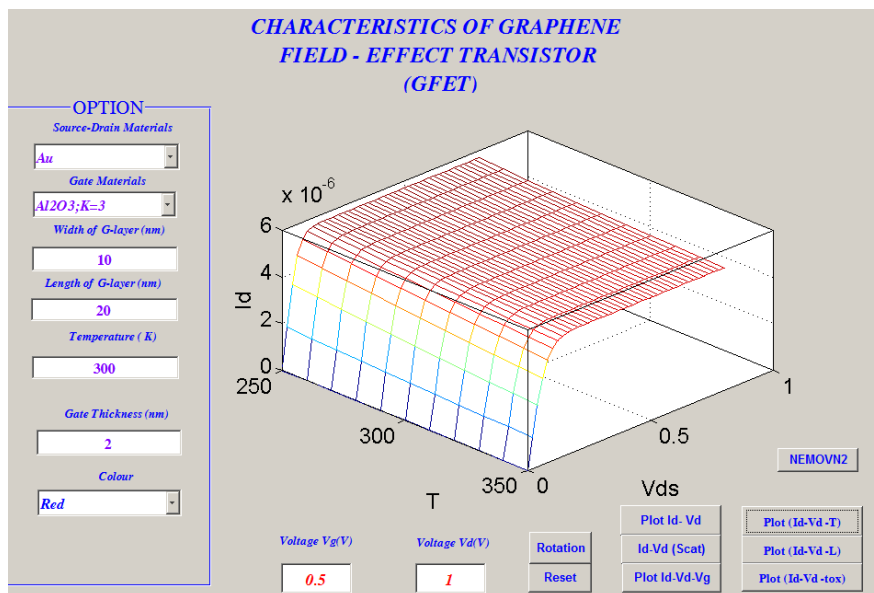
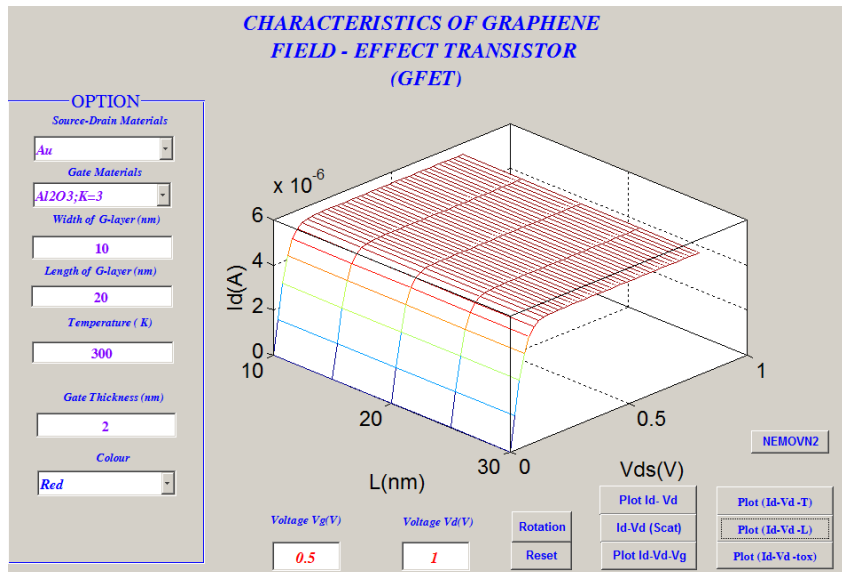


Fig. 5. The 3D plot of the  $I_D$ - $V_D$  characteristics of the top gate graphene FET vs temperature. The graphene FET parameters are: material, Al<sub>2</sub>O<sub>3</sub>, the gate length is  $L_G = 20$  nm, the gate thickness is  $t_{ox}=2$  nm.

Fig. 6 demonstrates  $I_D$ - $V_D$  characteristics of graphene FET versus the length of the gate layer at room temperature. When the length of the FET

is increased the saturated drain current is gradually decreased.



**Fig. 6.** The 3D plot of the  $I_D$ - $V_D$  characteristics vs the gate length of the top gate graphene FET at room temperature,  $T = 300$  K. The parameters of the graphene FET: material,  $Al_2O_3$ , the gate thickness,  $t_{ox} = 2$  nm.

Fig. 7 shows  $I_D$ - $V_D$  characteristics of the top gate graphene FET versus the gate thickness at room temperature. When the gate thickness,  $t_{ox}$  of

the graphene FET is increased the saturated drain current is gradually decreased.

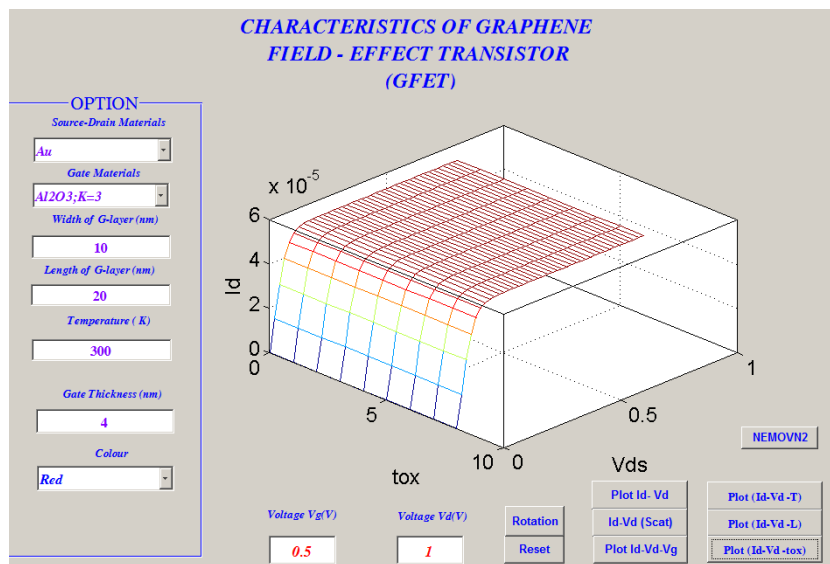


**Fig. 7.** The 3D plot of  $I_D$ - $V_D$  characteristics of the graphene FET vs the gate thickness,  $t_{ox}$  at room temperature,  $T = 300$  K. The parameters of the graphene FET: material,  $Al_2O_3$ , the gate length is  $L_G = 20$  nm.

**CONCLUSION**

A model for the graphene FET using NEGF written in GUI of Matlab has been reported. The top-gated graphene FET has been simulated. Typical simulations is then successfully performed for various parameters of the graphene FET. The modeling results agree with the experimental data. The model is not only able to accurately describe  $I_D$ - $V_G$ ,  $I_D$ - $V_D$  characteristics

of the graphene FET, but also affects of channel materials, gate materials, size of graphene FET, temperature on the characteristics. The simulation program is a good tool for the development and investigation of quantum device such as the graphene FET.

*ACKNOWLEDGMENTS:* This work is supported by VNU in HCM City under research contract NO. B2010-18-28.

# Mô phỏng đặc trưng dòng-thế của graphene FET

## • Đinh Sỹ Hiền

Trường Đại học Khoa học Tự nhiên, ĐHQG-HCM

**TÓM TẮT**

Chúng tôi đã phát triển chương trình mô phỏng transistor trường graphene cổng trên (GFET). Trong công trình này, chúng tôi tổng quan về vật liệu graphene, graphene FET. Chúng tôi sử dụng chương trình mô phỏng này để nghiên cứu kỹ đặc tính của graphene FET. Mô hình của graphene FET dựa trên

phương pháp hàm Green không cân bằng và lần đầu tiên được hiện thực bằng sử dụng giao diện đồ họa người sử dụng (GUI) của Matlab. Những đặc trưng dòng-thế của GFET, ảnh hưởng của vật liệu, nhiệt độ, thế cổng cũng được nghiên cứu kỹ.

**Từ khóa:** Graphene, graphene FET, hàm Green không cân bằng, đặc trưng dòng-thế.

**REFERENCES**

- [1]. K.S. Novoselov, A.K. Geim, S.V. Morozov, D. Jiang, Y. Zhang, S.V. Dubonos, I.V. Grigorieva, and A.A. Firsov, Electric field effect in atomically thin films, *Science*, 306, 666-669 (2004).
- [2]. L. Jiao, L. Zhang, X. Wang, G. Diankov, and H. Dai, Narrow graphene nanoribbons from carbon nanotubes, *Nature*, 458, 877-880 (2009).
- [3]. X. Li, X. Wang, L. Zhang, S. Lee, H. Dai, Chemically driven, ultrasmooth graphene nanoribbon semiconductors, *Science*, 319, 1229-1232 (2008).
- [4]. K.I. Bolotin, K.J. Sikes, Z. Jiang, G. Fundenberg, J. Hone, P. Kim, and H.L. Stormer, Ultrahigh electron mobility in suspended graphene, *Solid State Comm.*, 146, 351-355 (2008).
- [5]. M.S. Purewal, Y. Zhang, P. Kim, Unusual transport properties in carbon based nanoscaled materials: nanotubes and graphene, *Phys. State Sol.(b)*, 243, 3418-3422 (2006).

- [6]. J.S. Moon, D. Curtis, M. Hu, D. Wong, P.M. Campbell, G. Jernigan, J.L. Tedesco B. Vanmil, R. Myers-Ward, C. Eddy, D.K Gaskill, Epitaxial graphene RF field-effect transistors on Si-face 6H-SiC substrates, *IEEE electron device Lett.*, 30, 650-652 (2009).
- [7]. Y.M. Lin, C. Dimitrakoponlos, K.A. Jenkins, D.B. Farmer, H.Y. Chiu, A. Grill, Ph. Avouris, 100-GHz transistors from wafer-scale epitaxial graphene, *Science*, 327, 662 (2010).
- [8]. Y.Q. Wu, P.D. Ye, M.A. Capano, Y. Xuan, Y. Sui, M. Qi, J.A. Cooper, T. Shen, D. Pandey, G. Prakash, R. Reifengerger, Top-gate graphene field effect transistors formed by decomposition of SiC, *Appl. Phys. Lett.*, 92, 092102 (2008).
- [9]. E.H. Hwang and S. Das Sarm, Dielectric function and plasmons in two-dimensional graphene, *Phys. Rev. B*, 75, 0205418 (2007).
- [10]. E.H. Hwang, S. Das Sarma, Acoustic phonon scattering limited carrier mobility in two-dimensional extrinsic graphene, *Phys. Rev. B*, 77, 115449 (2008).
- [11]. J.H. Chen, C. Jang, S. Xiao, M. Ishigami, M.S. Fuhrer, Intrinsic and extrinsic performance limits of graphene devices on SiO<sub>2</sub>, *Nat. Nanotech.*, 3, 206-209 (2008).
- [12]. T. Ando, Screening effect and impurity scattering in monolayer graphene, *J. Phys. Soc. Japan*, 074716 (2006).
- [13]. I. Meric, M.Y. Han, A.F. Young, B. Oezylmaz, P. Kim, K. Shepard, Current saturation in zero-bandgap top-gated graphene field-effect transistors, *Nat. Nanotech.*, 3, 654-659 (2008).
- [14]. I. Meric, C. Dean, A.F. Young, J. Hone, P. Kim, K. Shepard, Graphene field-effect transistors based on boron nitride gate dielectrics, *IEDM Tech. Dig.*, 556-559 (2010).
- [15]. M. Freitag, M. Steiner, Y. Martin, V. Perebeinos, Z. Chen, J.C. Tsang, P. Avouris, Energy dissipation in graphene field effect transistors, *Nano Lett.*, 9, 1883-1888 (2009).
- [16]. V.E. Dorgan, M.H. Bae, E. Pop, Mobility and saturation velocity in graphene on SiO<sub>2</sub>, *Appl. Phys. Lett.*, 97, 082112 (2010).
- [17]. V. Perebeinos, P. Avouris, Inelastic scattering and current saturation in graphene, *Phys. Rev. B*, 81, 195442 (2010).
- [18]. A.M. Dasilva, R. Zou, J.K. Jain, J. Zhu, Mechanism for current saturation and energy dissipation in graphene transistors, *Phys. Rev. Lett.*, 104, 236601 (2010).
- [19]. X. Li, E.A. Barry, J.M. Zavada, M. Buongiorno Nardelli, K.W. Kim, Surface polar phonon dominated electron transport in graphene, *Appl. Phys. Lett.*, 97, 232105 (2010).
- [20]. J. Chauhan, J. Guo, High-field transport and velocity saturation in graphene, *Appl. Phys. Lett.*, 95, 023120 (2009).
- [21]. R.S. Shishin, D.K. Ferry, Velocity saturation in intrinsic graphene, *J. Phys. Condens. Matter*, 21, 344201 (2009).
- [22]. S. Datta, *Quantum Transport: Atom to Transistor*, Cambridge University Press (2005).
- [23]. S. Kim, J. Nah, I. Jo, D. Shahrjerdi, L. Colombo, Z. Yao, E. Tuctuc, S.K. Banerjee, Realization of a high mobility dual-gated graphene FET with Al<sub>2</sub>O<sub>3</sub> dielectric, *Appl. Phys. Lett.*, 94, 062107 (2009).